

Supporting Information for

“Forest aboveground biomass stock and resilience in a tropical landscape of Thailand.”

Authors: Nidhi Jha, Nitin Kumar Tripathi, Wirong Chanthorn, Warren Brockelman, Anuttara Nataland, Raphaël Pélissier, Siriruk Pimmasarn, Pierre Ploton, Nophea Sasaki, Salvatore Virdis, Maxime Réjou-Méchain

Table S1. Lidar metrics (n = 21) and their descriptions

Performance comparisons of several LiDAR-derived metrics to infer AGB at 0.5-ha resolution. Metrics (1-17) were calculated directly from the LiDAR cloud dataset and metrics (18-21) were derived from the canopy height model (CHM), which itself derived from the LiDAR cloud data. LOOCV-RMSE is the back-transformed error of the LiDAR-AGB log-log model obtained through a leave-one-out scheme (see methods). The relative RMSE is the ratio of this LOOCV-RMSE to the mean of field AGB.

| <i>S.No.</i> | <i>LiDAR metric</i> | <i>LOOCV-RMSE</i> | <i>Relative RMSE (in%)</i> |
|--------------|--|-------------------|----------------------------|
| 1 | H ₁₀ (10 th Percentile) | 93.53 | 29.70 |
| 2 | H ₂₅ (25 th Percentile) | 72.13 | 22.90 |
| 3 | H ₅₀ (50 th Percentile) | 48.73 | 15.47 |
| 4 | H ₇₅ (75 th Percentile) | 50.08 | 15.90 |
| 5 | H ₉₅ (95 th percentile) | 67.78 | 21.52 |
| 6 | H _{IQR} (HIQR = Q75 - Q25) | 81.02 | 25.72 |
| 7 | H _{mean} | 47.16 | 14.97 |
| 8 | H _{sqmean} (quadratic mean) | 48.44 | 15.38 |
| 9 | H _{cv} coefficient of variation of all height | 94.79 | 30.10 |
| 10 | Bin95 (Percent of points within Q95) | 93.95 | 29.83 |
| 11 | Bin75 (Percent of points within Q75) | 96.51 | 30.64 |
| 12 | Bin50 (Percent of points within Q50) | 95.54 | 30.33 |
| 13 | Bin25 (Percent of points within Q25) | 95.51 | 30.32 |
| 14 | Hperc10 Percentage of height ranges in 0–10m | 91.76 | 29.13 |
| 15 | Hperc20 Percentage of height ranges in 0–20m | 74.45 | 23.64 |
| 16 | Hperc30 Percentage of height ranges in 0–30m | 74.98 | 23.81 |
| 17 | Hperc40 Percentage of height ranges in 0–40m | 89.75 | 28.50 |
| 18 | TCH (Mean of top of Canopy Height) | 45.2 | 14.35 |
| 19 | CHM_H50 | 47.8 | 15.18 |
| 20 | CHMH _{relief} (((mean - min) / (max - min)) | 90.12 | 28.61 |
| 21 | CHMSqMean | 46.83 | 14.87 |

Table S2. Results from the model selection approach using TCH and any other of the additional LiDAR-based metrics described in Table S1 in a log-log linear model of the form $\log(AGB) = a + b \times \log(TCH) + c \times \log(X)$, where X is the additional metric tested given in the table. LOOCV-RMSE is the back-transformed error of this model obtained through a leave-one-out scheme (see methods). The relative RMSE is the ratio of the LOOCV-RMSE to the mean of field AGB. Adding a second predictor did not reduce the relative LOOCV-RMSE by more than 1, so only TCH was selected as final predictor.

| Log- Log Model | LOOCV-RMSE RMSE | Relative RMSE Relative to mean AGB |
|-----------------------------------|----------------------------|---|
| AGB~TCH | 45.2 | 14.35% |
| AGB~ TCH + B95 | 44.90 | 14.26% |
| AGB~ TCH + B95+H10 | 43.86 | 13.96% |
| AGB~ TCH + B95+H10+Hperc40 | 45.11 | 14.32% |

Table S3: Landsat Time-series data used for the study with corresponding validation score

| S.No | Landsat Mission | Sensor | Date of collection | Validation Score |
|-------------|------------------------|---------------|---------------------------|-------------------------|
| 1 | Landsat 1-3 | MSS | 19/12/1972 | 94.12 |
| 2 | Landsat 1-3 | MSS | 6/1/1973 | 90.69 |
| 3 | Landsat 1-3 | MSS | 13/12/1975 | 92.65 |
| 4 | Landsat 1-3 | MSS | 18/01/1976 | 94.12 |
| 5 | Landsat 1-3 | MSS | 18/11/1978 | 94.61 |
| 6 | Landsat 1-3 | MSS | 1/12/1979 | 96.57 |
| 7 | Landsat 1-3 | MSS | 13/01/1982 | 95.1 |
| 8 | Landsat 4-5 | TM | 9/12/1987 | 94.61 |
| 9 | Landsat 4-5 | TM | 11/12/1988 | 96.57 |
| 10 | Landsat 4-5 | TM | 13/02/1989 | 96.08 |
| 11 | Landsat 4-5 | TM | 5/4/1990 | 98.53 |
| 12 | Landsat 4-5 | TM | 2/11/1991 | 97.06 |
| 13 | Landsat 4-5 | TM | 18/03/1992 | 95.1 |
| 14 | Landsat 4-5 | TM | 23/11/1993 | 96.08 |
| 15 | Landsat 4-5 | TM | 28/12/1994 | 94.12 |
| 16 | Landsat 4-5 | TM | 20/03/1996 | 96.08 |
| 17 | Landsat 4-5 | TM | 20/12/1997 | 91.67 |
| 18 | Landsat 4-5 | TM | 23/12/1998 | 92.65 |
| 19 | Landsat 4-5 | TM | 26/12/1999 | 96.08 |
| 20 | Landsat 4-5 | TM | 12/12/2000 | 95.1 |
| 21 | Landsat 4-5 | TM | 2/3/2001 | 94.61 |
| 22 | Landsat 4-5 | TM | 24/01/2002 | 97.06 |
| 23 | Landsat 4-5 | TM | 21/11/2004 | 97.55 |
| 24 | Landsat 4-5 | TM | 13/03/2005 | 98.04 |
| 25 | Landsat 4-5 | TM | 13/12/2006 | 94.61 |
| 26 | Landsat 4-5 | TM | 30/01/2007 | 95.1 |
| 27 | Landsat 4-5 | TM | 18/12/2008 | 94.12 |
| 28 | Landsat 4-5 | TM | 19/11/2009 | 92.65 |
| 29 | Landsat 4-5 | TM | 25/01/2011 | 95.59 |
| 30 | Landsat 8 | OLI & TIRS | 30/11/2013 | 89.71 |
| 31 | Landsat 8 | OLI & TIRS | 19/12/2014 | 93.14 |
| 32 | Landsat 8 | OLI & TIRS | 2/4/2015 | 91.67 |
| 33 | Landsat 8 | OLI & TIRS | 11/3/2016 | 95.1 |
| 34 | Landsat 8 | OLI & TIRS | 25/01/2017 | 96.57 |

Figures

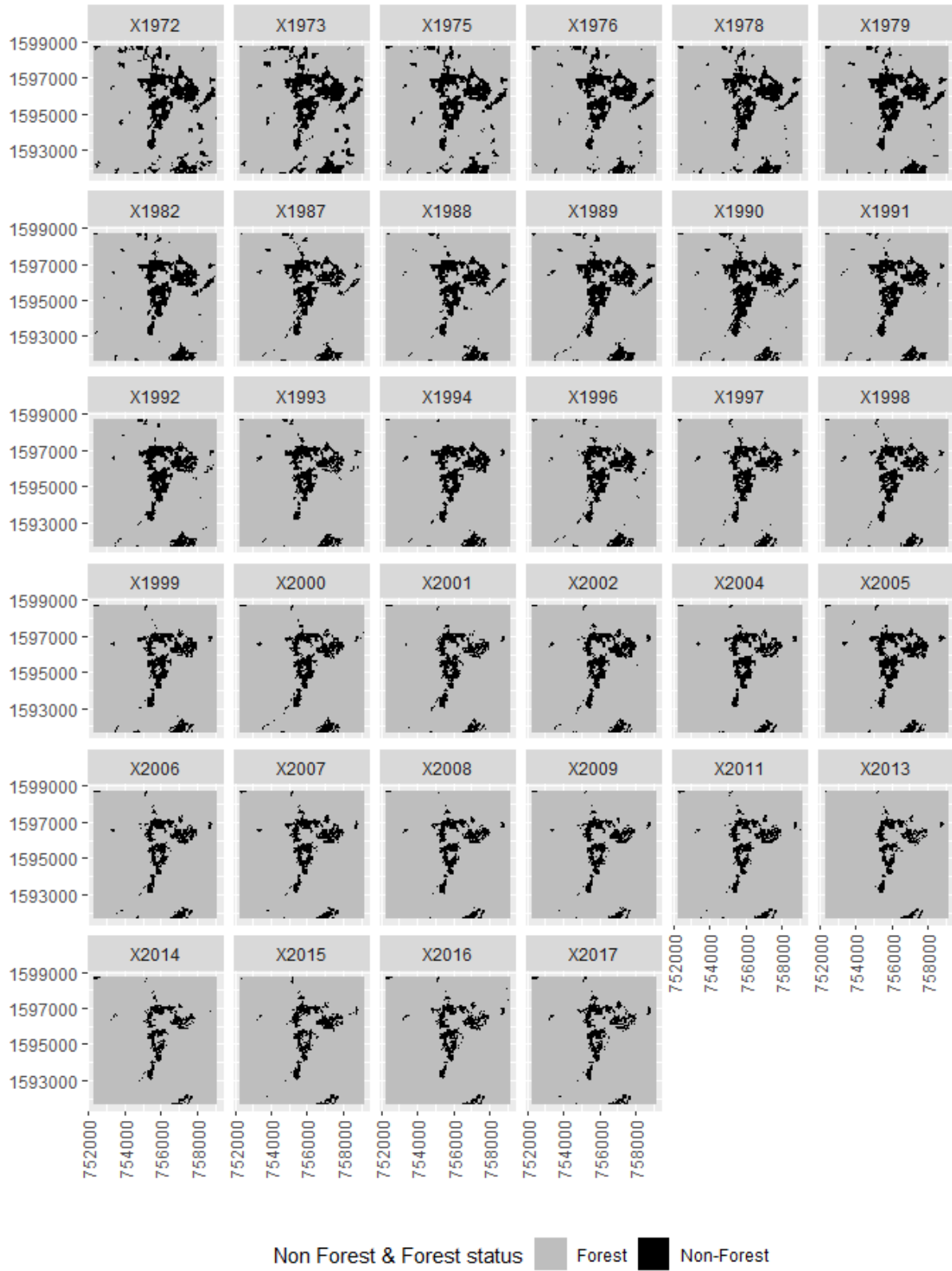


Fig S1: Non-Forest and Forest status across period (1972-2017)

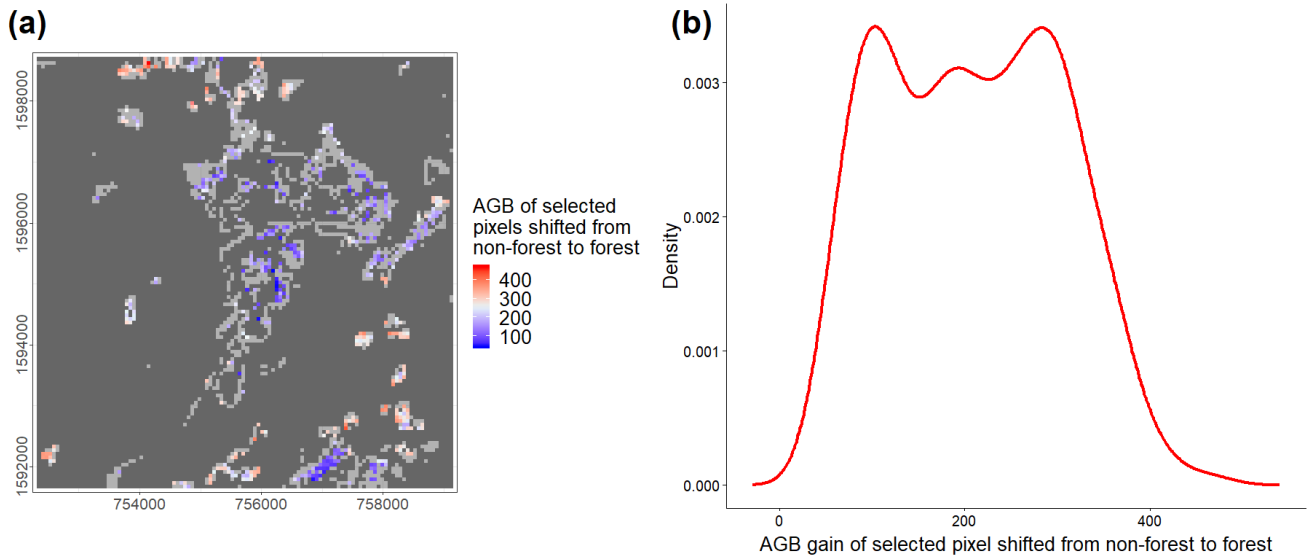


Fig S2: AGB recovery of the pixels that experienced a single shift from Non-Forest to Forest. (a)- Map showing spatialized single shifts from non-forests to forests with the corresponding AGB gain in 2017 as predicted by our LiDAR AGB map (Fig. 3a). Dark grey represents pixels that did not experience any shift and light grey represents pixels which did not pass our quality procedure during the study period. (b)- Density distribution of pixels with AGB gain which experiences single shifts over the landscape during the study period.

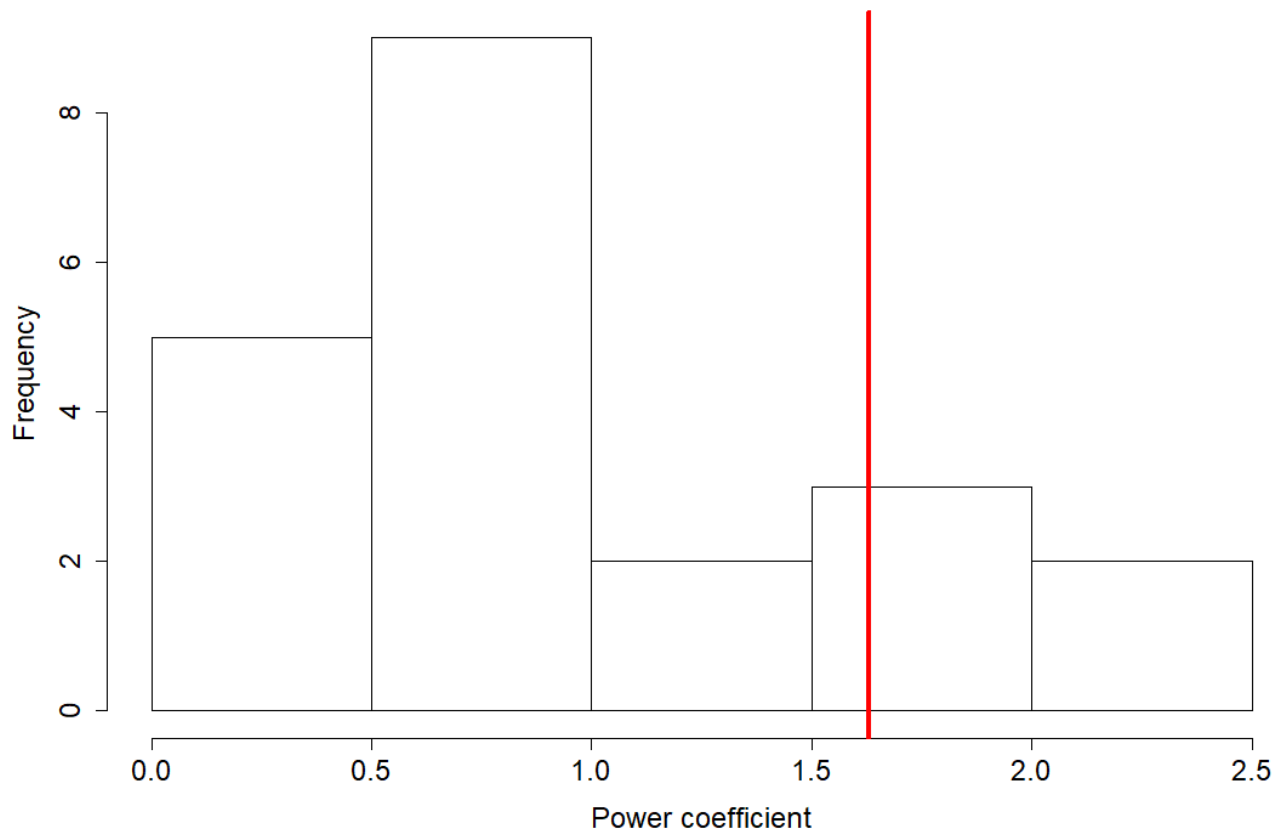


Fig S3: Distribution of the power coefficients obtained from site-specific power models fitted on AGB recovery versus forest age in 21 sites studied by Poorter et al. (2016) and in our site (red line). We only considered the sites having a minimum of 10 observations and that were younger than 45 years old. We excluded 7 sites matching those rules as they exhibited dubious patterns of carbon recovery through time that cannot be captured by a power model (sites Eastern Pará 2, El Carite, Mata Seca, Patos, San Carlos, Yucatán, Zona Norte).

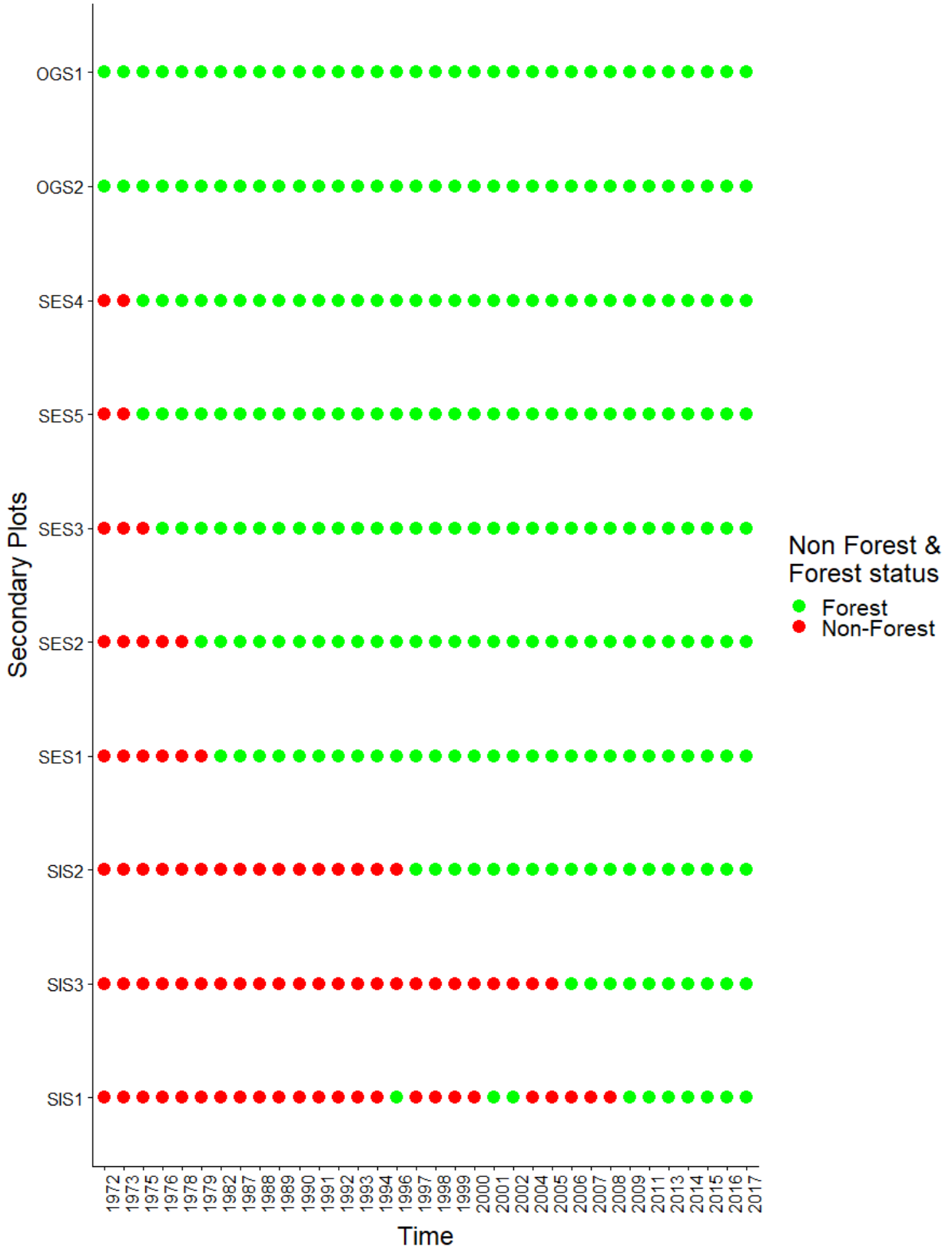


Fig S4. Non-forest (red) to forest (green) status during the 1972-2017 period in 10 field plots belonging to different successional stages as estimated from our forest classification approach. We did not represent here the subplots belonging to the Mo Singto plot as they all were in a forested status during the whole study period.